

DEVELOPMENT AND IMPLEMENTATION OF BUNCH SHAPE INSTRUMENTATION FOR ION LINACS*

S. A. Gavrilov[†], A. V. Feschenko, V. A. Gaidash,

Institute for Nuclear Research of the Russian Academy of Sciences, Moscow, Troitsk, Russia

Abstract

A longitudinal charge distribution in beam bunches, so-called bunch shape, is one of the most important and difficult to measure characteristics of a beam in ion linear accelerators. Despite the variety of approaches only the methods using low energy secondary electrons emitted, when the beam passes through a thin target, found practical application. The most common beam instrumentation, based on this method, became Bunch Shape Monitor (BSM) developed in INR RAS. The monitor provides direct measurements of bunch shape and bunch longitudinal halo, allows to carry out such complex diagnostic procedures as longitudinal emittance measurements, amplitude and phase setting of accelerating fields and observation of bunch shape evolution in time to check the overall quality of longitudinal tuning of the accelerator.

The principle of the monitor operation, design features, ultimate parameters and limitations are discussed. Several modifications of the monitor with implementation peculiarities are described as well as lots of measurement results at different ion linacs with a variety of beam parameters. New challenges for bunch shape instrumentation to satisfy demands of forthcoming linacs are also characterized.

INTRODUCTION

The main requirement for bunch shape measurements is phase resolution. In ion linacs for typical bunch phase duration range from several degrees to several tens of degrees the resolution of 1° looks adequate. The corresponding temporal resolution, for example for 350 MHz, equals to ~8 ps.

In ion beams, as opposite to electron ones, an attempt to extract information on bunch shape through beam electromagnetic field results in aggravation of phase resolution due to large longitudinal extent of the particle field. The problem can be overcome if one localizes a longitudinal space passing through which the bunch transmits information on its shape.

This approach can be implemented if a longitudinally small target is inserted into the beam and some type of radiation due to interaction of the beam with this target is detected. Different types of radiation are used or proposed to be used [1-5], however low energy secondary electrons are used most extensively. The distinctive feature of these electrons is a weak dependence of their properties both on type and energy of primary particles, so the detectors can be used for almost any ion beam.

Among the characteristics of low energy secondary emission, influencing the parameters of the bunch shape monitor, one can point initial energy and angular distributions as well as time dispersion or delay of the emission. Time dispersion establishes a fundamental limitation on the resolution of the detector. The value of time dispersion for metals is estimated theoretically to be about $10^{-15} \div 10^{-14}$ s [6], which is negligible from the point of view of bunch shape measurements. The experimental results of time dispersion measurements give not exact value but its upper limit. It was shown that the upper limit does not exceed $(4 \pm 2) \cdot 10^{-12}$ s [7].

Operation of bunch shape monitors with low energy secondary electrons is based on coherent transformation of a time structure of the analyzed beam into a spatial distribution of secondary electrons through RF modulation. The first real detectors described in [8, 9] use RF modulation in energy or in other words a longitudinal modulation. Another possibility is using a transverse scanning [10]. The electrons are modulated in transverse direction and deflected depending on their phase. Spatial separation is obtained after a drift space.

BUNCH SHAPE MONITOR OF INR RAS

Principle of Operation

The first real BSM with transverse scanning of low energy secondary electrons, developed and fabricated in INR, has been described in [11, 12].

The operation principle of BSM with up-to-date design can be described briefly with the reference to Fig. 1.

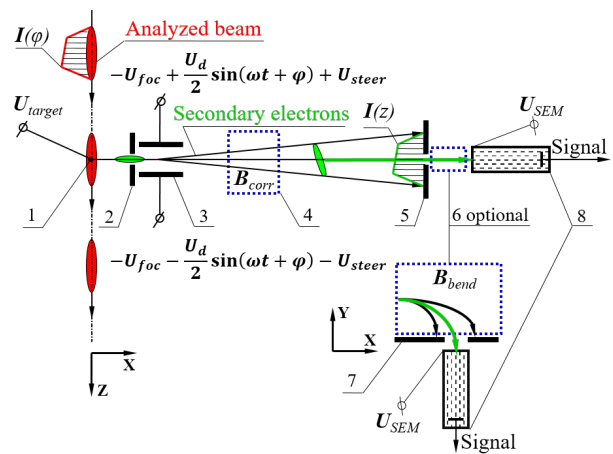


Figure 1: BSM scheme: 1 – tungsten wire target, 2 – inlet collimator, 3 – RF-deflector, 4 – correcting magnet, 5 – outlet collimator, 6 – optional bending magnet, 7 – registration collimator, 8 – electron detector.

* Work was awarded the Veksler Prize 2021 of RAS

[†] s.gavrilov@gmail.com

The series of bunches of the beam under study crosses the wire target 1 which is at a high negative potential (U_{target} about -10 kV). The target represents a tungsten wire of 0.1 mm diameter. Interaction of the beam with the target results in emission of low energy secondary electrons. The electrons are accelerated by electrostatic field and move almost radially away from the target. A fraction of the electrons passes through input collimator 2 and enters RF deflector 3 operating at a frequency equal to or multiple of the linac accelerating field frequency. Deflection of the electrons at the exit of the RF deflector depends on their phase with respect to deflecting field. Downstream of the drift distance the electrons are spatially separated and their coordinates are dependent on phase of the deflecting field. Temporal structure of the analyzed ion beam is initially transformed into that of secondary electrons and then into spatial distribution of the electrons. The intensity of the electrons at a fixed coordinate is proportional to the intensity of the primary beam at a fixed point along the bunch. These electrons are separated by outlet collimator 5 and their intensity is measured with electron detector 8. Adjusting the deflecting field phase with respect to accelerator RF reference, one can obtain a longitudinal distribution of charge in the bunches of the analyzed beam.

Main Parameters

The most important characteristic of BSM is its phase resolution. We define phase resolution by a simple relation $\Delta\varphi = \frac{\Delta Z}{nZ_{max}}$, where Z_{max} is the amplitude of electron displacement at collimator 5 plane, n is a harmonic number of the deflecting field with respect to the fundamental bunch array frequency and ΔZ is a full width at a half maximum of the electron beam at the collimator 5 for zero phase duration bunches of the analyzed beam. To decrease ΔZ and hence to improve the resolution the electron beam must be focused by additionally applying focusing potential U_{foc} to the deflector electrodes. To steer the electron beam additional potential difference U_{steer} is also applied between the deflector electrodes. Evidently the size of the collimator should not exceed ΔZ . Otherwise the size of the collimator is to be used in the above formula instead of electron beam size ΔZ .

The value of maximum displacement Z_{max} can be both calculated and found experimentally. As for the ΔZ value, its finding is not a trivial task. To find the value of ΔZ for the purpose of phase resolution evaluation both theoretical and experimental data are used. Initially focusing properties of the detector can be found experimentally using thermal electrons. Heating the wire target made of tungsten, it is possible to visually observe the thermal electron beam on the phosphor covering the front surface of the plates of collimator 5 through the viewing port. The size of the focused beam of secondary electrons can be measured by adjusting the steering

voltage U_{steer} for the turned off RF deflecting field. After that computer simulations can be done to find the value of ΔZ for real parameters of the low energy secondary electrons taking into account a real spatial distribution of the deflecting field. Sometimes instead of full width at a half maximum a double rms size is used.

Another important characteristic is an ability of measuring small intensities. This feature is especially important for longitudinal halo measurements. Using a secondary electron multiplier as an electron beam detector 8 enables the measurements to be done within 5 orders of intensity magnitude.

The limitation of BSM use for high intensities is due to two reasons. The first one is target heating. In case of tungsten target before its destruction the overheating is manifested as arising of thermal electron current. A bunch substrate increasing within the beam pulse is observed when bunch behaviour within the beam pulse is measured.

The second limitation is effect of space charge of the analysed beam.

Influence of Analyzed Beam Space Charge

All the estimations described above are done with the assumption of a zero-intensity analysed beam, while a space charge of the real beam can strongly influence the secondary electrons trajectories and result in phase resolution deterioration [13-14].

As an example, the results of simulations for ESS proton linac for different beam currents are presented in Fig. 2. The phase resolution is given as a function of a longitudinal coordinate along the bunch. The bunch head is at the left side in the figure.

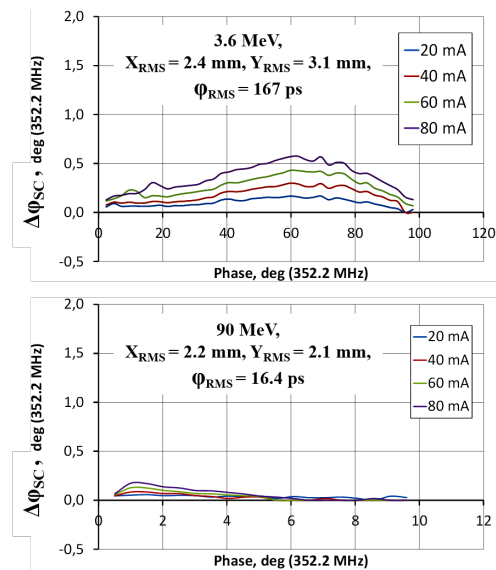


Figure 2: Space charge effect for various beam currents.

Also the energy modulation of secondary electrons by the space charge can result in a phase reading error, when the measured phase coordinate along the bunch does not correspond to the real one.

MODIFICATIONS OF BUNCH SHAPE MONITOR

Additionally to the basic detector above described there are three BSM modifications: BSM for H^- beams, Bunch Length and Velocity Detector (BLVD) and Three Dimensional Bunch Shape Monitor (3D-BSM).

BSM for H^- Minus Beams

In case of H^- beam a fraction of the detached electrons after interaction with the BSM target gets into the secondary electron channel of BSM and the detected signal represents a superposition of signals due to low energy secondary electrons and the detached electrons. The effect has been analyzed in [15]. The energy of the detached electrons differs from that of low energy secondary electrons so the two groups of the electrons can be effectively separated. BSM for H^- beam includes additional element – bending magnet located between the outlet collimator and the electron detector.

Bunch Length and Velocity Detector

BLVD is a BSM, which can be mechanically translated along the beam line [16]. In this detector a time of flight method of energy measurements is implemented. The translation results in a shift in phase of the observed distribution. Measuring the value of the translation and the value of the shift one can find an average velocity of the beam. The accuracy of bunch shape measurements for this detector is the same as for normal BSM. Special procedure of velocity measurement enables to decrease systematic error to $\pm 0.1\%$. Total error of velocity measurements is typically within $\pm(0.3\div 0.4)\%$.

Three-Dimensional Bunch Shape Monitor

3D-BSM is aimed to measure a three-dimensional distribution of charge in bunches [17]. Due to high strength and concentration of electric field near the wire target the electrons move almost perpendicular to its axis with very small displacement along the wire in the area between the target and the input collimator. Additional slit perpendicular to the target installed outside the beam enables to separate the secondary electrons emitted from a fixed coordinate along the wire. For fixed position of the wire and fixed position of the additional slit the intensity of the electrons passed through the slit is proportional to beam intensity at the fixed transverse coordinate. The phase distribution of the separated electrons is measured in the same manner as in basic BSM. Moving the target and the slit and each time measuring longitudinal distribution one can obtain a three-dimensional distribution of charge in bunches.

COMMISSIONING EXPERIENCE

The first BSM with transverse scanning of low energy secondary electrons has been developed and built in INR in the eighties and the first measurements has been done in 1988 during commissioning of INR linac. Since that time BSMs of various modifications have been developed

and built for several accelerators (Table 1). It should be noted that the detectors of this type have also been developed in other laboratories [18-20].

Table 1: BSM Commissioning History

Year	LINAC	Beam commissioning	Quantity
1988	INR RAS	H^+ (20, 100 MeV)	1 BSM
1993	SSC RFQ	H^+ (2.5 MeV)	1 BSM
1994	CERN LINAC3	Pb^{27+} (0.25, 4.2 MeV/u)	1 BLVD
1996	CERN LINAC2	H^+ (50 MeV)	1 3D-BSM
1996	JHP RFQ	H^+ (3 MeV)	1 BLVD
1997	DESY	H^- (10, 30, 50 MeV)	2 BSMs + 1 BLVD
1997	INR RAS	H^+ (160 MeV)	1 BLVD
1999-2000	CERN LINAC2	H^+ (10, 30 MeV)	2 BSMs
2003-2010	SNS ORNL	H^- (7.5, -90, -180, -1000 MeV)	8 BSMs
2012-2016	CERN LINAC4	H^- (3+160 MeV)	2 BSMs
2012	J-PARC	H^- (~200 MeV)	3 BSMs
2016	LANSCE	H^+ , H^- (0.75, ~70 MeV)	2 BSMs
2016	GSI-FAIR	Ar^{26+} (3.5 MeV/u)	1 BSM
2019	FRIB	Ar^{26+} (20 MeV/u)	1 BSM
2021	GSI-FAIR	Ar^{26+} (1.4+7 MeV/u), H^+ (3+70 MeV)	2 BSMs
2022	ESS	H^+ (3.6, 90 MeV)	2 BSMs
2022	MYRRHA	H^+ (1.5, 5.9 MeV)	1 BSM

MAIN BSM COMPONENTS

Typical BSM components [21] are RF and HV systems, secondary electron detection system, control system as well as magnetic shield and corrector.

RF System

The system includes RF deflector, RF amplifier and phase shifter. Depending on BSM design features both fundamental bunch array frequency and higher harmonics are used. The deflector is combined with the electrostatic lens thus enabling simultaneous focusing and RF-scanning of the electrons. Typically, BSM deflectors are RF-cavities, based on parallel wire lines with capacitive plates. An electrical length of the deflectors is usually $\lambda/4$ or $\lambda/2$. To improve the uniformity of both deflecting and focusing fields in Y-direction, thus improving a phase resolution, the new λ -type symmetric cavity has been developed for BSM-ESS [22]. The uniformity of the field in a zone of the electron beam passage is an order of magnitude better for the symmetric type (Fig. 3).

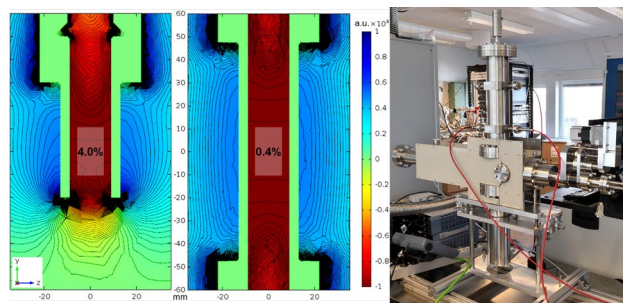


Figure 3: RF-field E_z -component distribution in YZ-plane of $\lambda/2$ - and λ -type BSM deflectors and photo of BSM-ESS with the implemented λ -type deflector.

Typical value of RF power required for deflector excitation is near 10 W and ~20 W for symmetric deflector type. Phase of the deflecting field is normally adjusted from pulse to pulse and the most suitable are voltage controlled electronic phase shifters.

Content from this work may be used under the terms of the CC BY 3.0 licence (© 2021). Any distribution of this work must maintain attribution to the author(s), title of the work, publisher, and DOI

HV System

The HV system is intended to supply HV potentials to the target and electrostatic lens as well as to secondary electron multiplier. Typical value of target potential is -10 kV. To provide BSM tuning with thermal electrons a filament source is foreseen at HV target potential. To provide steering of the electrons an adjustable voltage difference of several hundred volts must be superimposed on focusing potential.

Electron Detection System

Secondary electron multipliers are most widely used. In this single channel system only one phase point is detected for a fixed phase setting hence multiple beam pulses are required for bunch shape measurement.

The detection system of 3D-BSM uses 30-channel electron collector thus enabling the measurement of the whole longitudinal distribution to be done per single beam pulse.

Control System

In principle any type of control system can be used. However the most recent our developments are based on LabVIEW platform with the use of National Instruments control modules NI USB-6363 and NI-9264.

Magnetic Shield and Corrector

Often BSMs are installed in a close vicinity of magnetic focusing elements with strong fringe fields both static and alternating. In this case a magnetic shield must be used to provide a non-distorted e-beam transport inside BSM. Typical BSM shield represents a sectional jacket made of low-carbon steel with interior surfaces covered with a foil made of a cobalt-iron alloy with high μ_r . Figure 4 shows the effect of the BSM shield on the fringe field of a quad located close to the BSM-ESS. Better results can be obtained if additional screens are added upstream and downstream of BSM. In this case the remnant fields decrease to the level less than the Earth's magnetic field, and their influence will be negligible.

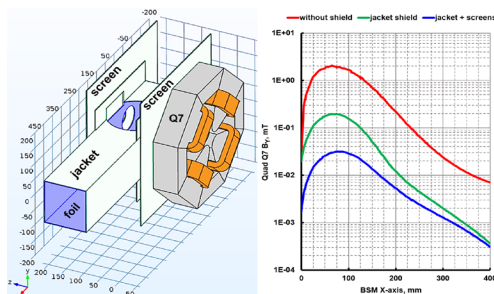


Figure 4: BSM shield design and the quad B_y distribution.

An influence of remnant static magnetic fields inside the standard shield as well as unavoidable misalignments can be compensated for Z-direction by adjusting the steering voltage U_{steer} and for other directions with the help of additional magnetic corrector with superposition of dipole and quadrupole magnetic fields [23]: the dipole

field moves the electron beam along Y-axis and the quadrupole field enables to adjust the tilt of the e-beam in YZ-plane (Fig. 5).

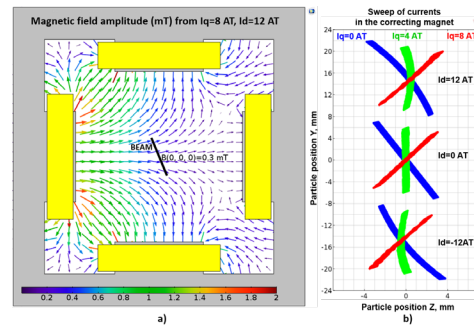


Figure 5: (a) Magnetic corrector with fields superposition. (b) E-beam in the plane of the outlet collimator for different quadrupole I_q and dipole I_d coil currents.

SOME EXPERIMENTAL RESULTS

Normally different phase points are measured for different beam pulses and the signal is digitized within the beam pulse. It is implied that bunches are reproducible from pulse to pulse though can vary within the beam pulses. BSM allows to observe an evolution of charge longitudinal distribution in bunches within a beam pulse. Figure 6 demonstrates an evolution of bunch shape observed at the initial stage of CERN Linac-4 commissioning, when the beam loading compensation was insufficient.

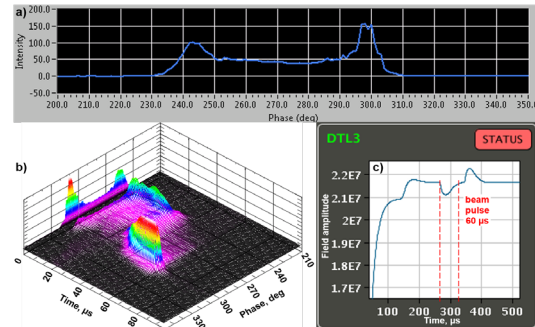


Figure 6: Experimental data from CERN Linac-4. a) A bunch shape with 1° resolution. b) Evolution of a bunch shape during a beam pulse. c) DTL3 field amplitude with the beam.

Data about evolution in time can be used as a generalized criterion of correct operation of all accelerator systems influencing on the longitudinal beam dynamics, including accelerating field parameters (Fig. 7).

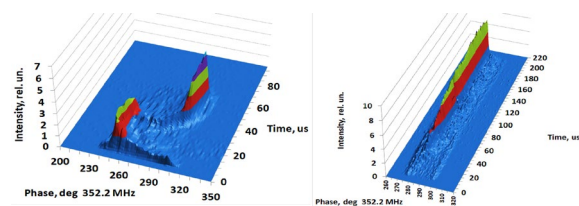


Figure 7: Behavior of bunch shape in time at the exit of CERN Linac-4 during commissioning (left) and for normal operation (right).

If the measurements are done with increased gains of secondary electron multiplier a longitudinal halo can be observed [24,25] (Fig. 8).

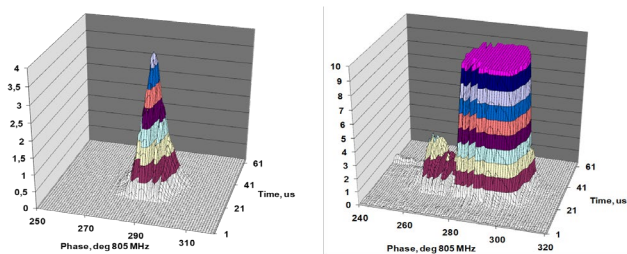


Figure 8: Observation of bunch longitudinal halo in the first SNS CCL: left – nominal SEM-gain, right – 160 times larger gain.

Bunch shape measurements can be used also for restoration of longitudinal emittance (Fig. 9), setting of accelerating field parameters, longitudinal matching etc.

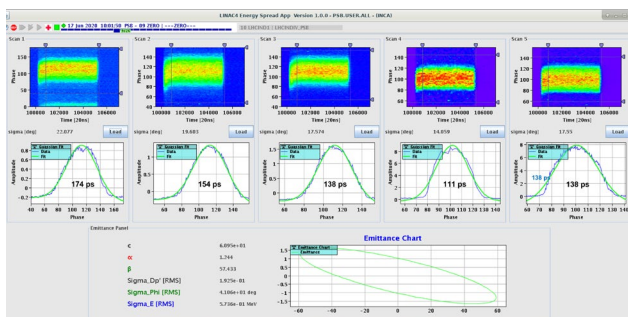


Figure 9: Longitudinal phase ellipse at the entrance of CERN PS Booster [26].

CONCLUSIONS

Bunch Shape Monitors being developed in INR RAS since eighties have become a new class of precise beam instrumentation for longitudinal beam parameters measurements and beam dynamics studies in ion linacs. They enable to obtain the results with the resolution unachievable with other conventional instrumentation. As an example Fig. 10 demonstrated the results of bunch shape measurements made with phase probes, fast current transformer and BSM [27].

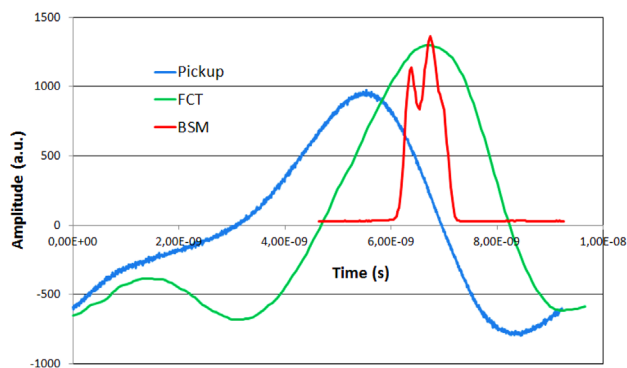


Figure 10: Bunch shapes of identical bunches of 3.5 MeV/u Ar⁹⁺ beam in GSI cw-Linac prototype measured with three different detectors.

REFERENCES

- [1] A. S. Artimov, A. K. Gevorkov, V. V. Limar, V. P. Sidorov, and N. G. Vaganov, “Method and Apparatus for Multifunctional Nonperturbing Diagnostics of H- Beams”, in *Proc. 14th Particle Accelerator Conf. (PAC’91)*, San Francisco, CA, USA, May 1991, pp. 1573-1576.
- [2] S. Assadi, “SNS Transverse and Longitudinal Laser Profile Monitors Design, Implementation and Results”, in *Proc. 10th European Particle Accelerator Conf. (EPAC’06)*, Edinburgh, UK, Jun. 2006, paper THPCH156, p. 3161.
- [3] Y. Liu *et al.*, “Laser Based Diagnostics for Measuring H-Beam Parameters”, in *Proc. 24th Particle Accelerator Conf. (PAC’11)*, New York, NY, USA, Mar.-Apr. 2011, paper WEOCN1, pp. 1433-1437.
- [4] P. N. Ostroumov, A. Barcikowski, A. Delannoy, S. A. Kondrashev, and J. A. Nolen, “Bunch Length Detector Based on X-Ray Produced Photoelectrons”, in *Proc. 23rd Particle Accelerator Conf. (PAC’09)*, Vancouver, Canada, May 2009, paper TU3GRC04, pp. 751-753.
- [5] P. Forck and C. Dorn, “Measurements with a Novel Non-Intercepting Bunch Shape Monitor at the High Current GSI-LINAC”, in *Proc. 7th European Workshop on Beam Diagnostics and Instrumentation for Particle Accelerators (DIPAC’05)*, Lyon, France, Jun. 2005, paper POM010, p. 48.
- [6] I. M. Bronstein, B. S. Fraiman, “Secondary Electron Emission”, Moscow, Nauka, 1969 (in Russian).
- [7] E. W. Ernst, H. V. Foerster, “Time dispersion of secondary emission”, *Journal of Appl. Phys.*, v. 26, No. 6, pp. 781-782, 1955.
- [8] R. L. Witkover, “A non-destructive bunch length monitor for a proton linear accelerator”, *Nucl. Instrum. Meth.*, v. 137, No. 2, pp. 203-211, 1976.
- [9] A. Tron, A. Feschenko, “A monitor of proton beam phase distribution in linear resonance accelerator”, in *Proc. 7th all union meeting on particle accelerators*, Dubna, USSR, 1981, v. 2, p. 125 (in Russian).
- [10] I. A. Prudnikov, USSR invention license, H05h7/00, No.174281 (in Russian).
- [11] A. V. Feschenko and P. N. Ostroumov, “Bunch Shape Measuring Technique and its Application for an Ion Linac Tuning”, in *Proc. 1986 Linear Accelerator Conf. (LINAC’86)*, Stanford, CA, USA, Jun. 1986, paper WE3-30, pp. 323-327.
- [12] A. V. Feschenko, P. N. Ostroumov, “Bunch shape measurements at the INR linac”, in *Proc. Workshop on Advanced Beam Instrumentation*, KEK, Tsukuba, Japan, April 1991, pp. 235-245.
- [13] A. V. Feschenko and V. A. Moiseev, “Space Charge Effects in Bunch Shape Monitors”, in *Proc. 20th Linear Accelerator Conf. (LINAC’00)*, Monterey, CA, USA, Aug. 2000, paper MOC13, p. 178.
- [14] A. Feschenko and V. A. Moiseev, “Peculiarities of Bunch Shape Measurements of High Intensity Ion Beams”, in *Proc. 1st Int. Particle Accelerator Conf. (IPAC’10)*, Kyoto, Japan, May 2010, paper MOPE041, pp. 1065-1067.
- [15] A. Denisov, A. Feschenko, and A. Aleksandrov, “Peculiarities Of Bunch Shape Measurements Of H-Minus Beams In Linear Accelerators”, in *Proc. 21st Russian Particle Accelerator Conf. (RuPAC’08)*, Zvenigorod, Russia, Sep.-Oct. 2008, paper WEEAU02, p. 298.

- [16] P. N. Ostroumov, A. V. Feschenko, V. A. Gaidach, S. A. Krioukov, A. A. Menshov, and A. Ueno, “Bunch Length and Velocity Measurement of the JHP-RFQ Beam with INR BLVD”, in *Proc. 19th Int. Linac Conf. (LINAC'98)*, Chicago, IL, USA, Aug. 1998, paper TH4061, pp. 905-907.
- [17] S. K. Esin *et al.*, “A three dimensional bunch shape monitor for the CERN proton linac”, in *Proc. 18th Linear Accelerator Conf. (LINAC'96)*, Geneva, Switzerland, Aug. 1996, paper MOP53, p. 193.
- [18] E. S. McCrory, C. W. Schmidt, and A. V. Feschenko, “Use of INR-Style Bunch-Length Detector in the Fermilab Linac”, in *Proc. 1992 Linear Accelerator Conf. (LINAC'92)*, Ottawa, Canada, Aug. 1992, paper TH4-21, pp. 662-664.
- [19] N. Y. Vinogradov *et al.*, “Bunch Shape Measurement of CW Heavy-Ion Beam”, in *Proc. 21st Linear Accelerator Conf. (LINAC'02)*, Gyeongju, Korea, Aug. 2002, paper MO411, pp. 61-63.
- [20] N. Y. Vinogradov *et al.*, “A detector of bunch time structure for cw heavy-ion beams”, *Nucl. Instrum. Meth. A* 526, p. 206, 2004.
- [21] S. Gavrilov *et al.*, “Bunch Shape Monitors for modern ion linacs”, *JINST* v. 12 p. 12014, 2017.
- [22] S. A. Gavrilov, D. A. Chermoshentsev, and A. Feschenko, “Development, Fabrication and Laboratory Tests of Bunch Shape Monitors for ESS Linac”, in *Proc. 7th Int. Beam Instrumentation Conf. (IBIC'18)*, Shanghai, China, Sep. 2018, pp. 407-409. doi:10.18429/JACoW-IBIC2018-WEPA17
- [23] S. A. Gavrilov and A. Feschenko, “Design and Development of Bunch Shape Monitor for FRIB MSU”, in *Proc. 6th Int. Beam Instrumentation Conf. (IBIC'17)*, Grand Rapids, MI, USA, Aug. 2017, pp. 179-181. doi:10.18429/JACoW-IBIC2017-TUPCC13
- [24] J. Tan, G. Bellodi, A. Feschenko, and S. A. Gavrilov, “Results from the CERN LINAC4 Longitudinal Bunch Shape Monitor”, in *Proc. 7th Int. Beam Instrumentation Conf. (IBIC'18)*, Shanghai, China, Sep. 2018, pp. 415-419. doi:10.18429/JACoW-IBIC2018-WEPA19
- [25] A. Feschenko *et al.*, “Longitudinal Beam Parameters Study in the SNS Linac”, in *Proc. 22nd Particle Accelerator Conf. (PAC'07)*, Albuquerque, NM, USA, Jun. 2007, paper THOAAB01, pp. 2608-2610.
- [26] J. Tan, “LINAC4 diagnostics experience during commissioning”, in *Proc. ARIES workshop “Experiences during hadron linac commissioning”*, Jan. 2021, <https://agenda.ciemat.es/event/1229/contributions/2276/>
- [27] T. Sieber *et al.*, “Bunch Shape Measurements at the GSI CW-Linac Prototype”, in *Proc. 9th Int. Particle Accelerator Conf. (IPAC'18)*, Vancouver, Canada, Apr.-May 2018, pp. 2091. doi:10.18429/JACoW-IPAC2018-WEPAK006